

Article

Enhancing the Grinding Efficiency of a Magnetite Second-Stage Mill through Ceramic Ball Optimization: From Laboratory to Industrial Applications

Caibin Wu¹, Zhilong Chen¹, Ningning Liao^{2,*}, Chong Zeng¹, Yihan Wang¹ and Jingkun Tian¹

¹ School of Resources and Environmental Engineering, Jiangxi University of Science and Technology, Ganzhou 341000, China; caibin.wu@jxust.edu.cn (C.W.); 17607072272@163.com (Z.C.); 18770775773@163.com (C.Z.); wyh3222482679@163.com (Y.W.); tjkkk@163.com (J.T.)

² Jiangxi Provincial Key Laboratory of Low-Carbon Processing and Utilization of Strategic Metal Mineral Resources, Jiangxi University of Science and Technology, Ganzhou 341000, China

* Correspondence: liaoningning@jxust.edu.cn

Abstract: Ceramic ball milling has demonstrated remarkable energy-saving efficiency in industrial applications. However, there is a pressing need to enhance the grinding efficiency for coarse particles. This paper introduces a novel method of combining media primarily using ceramic balls supplemented with an appropriate proportion of steel balls. Three grinding media approaches, including the utilization of steel balls, ceramic balls, and a hybrid combination, were investigated. Through an analysis of the grinding kinetics and the R–R particle size characteristic formulas, the study compares the breakage rate and particle size distribution changes for the three setups. The results indicate that employing binary media effectively improves the grinding efficiency for +0.3 mm coarse particles while maintaining the energy-saving advantages of ceramic ball milling. Simultaneously, the uniformity of the ground product is ensured. This proposed approach has been successfully validated in industrial applications, providing robust theoretical support for the expansion of ceramic ball milling applications.

Keywords: ceramic ball; binary media; energy-saving; industrial application; magnetite



Citation: Wu, C.; Chen, Z.; Liao, N.; Zeng, C.; Wang, Y.; Tian, J. Enhancing the Grinding Efficiency of a Magnetite Second-Stage Mill through Ceramic Ball Optimization: From Laboratory to Industrial Applications. *Minerals* **2024**, *14*, 160. <https://doi.org/10.3390/min14020160>

Academic Editors: Josep Oliva and Hernán Anticoi

Received: 21 December 2023

Revised: 29 January 2024

Accepted: 29 January 2024

Published: 31 January 2024



Copyright: © 2024 by the authors. Licensee MDPI, Basel, Switzerland. This article is an open access article distributed under the terms and conditions of the Creative Commons Attribution (CC BY) license (<https://creativecommons.org/licenses/by/4.0/>).

1. Introduction

Grinding is an essential operation in the development and utilization of mineral resources, and it undertakes the important task of providing a suitable feed size for the subsequent beneficiation operation [1]. Ball mills are widely used in all stages of ore processing plants, and the grinding medium of choice in most mines is steel balls. While the traditional steel ball milling process has the advantage of high production capacity, it also has the disadvantages of over-grinding, iron contamination, and high energy consumption [2–4]. The energy consumption of grinding accounts for about 50% of the mineral processing plant, and it even exceeds 70% in some magnetic separation plants [5]. Given the current focus on carbon peaking, carbon neutrality goals, and rational electricity production in China, enterprises are now emphasizing energy savings and green development more than ever before. For heavy industrial enterprises such as mines, energy-saving efforts, cost reduction, and efficiency enhancement have become particularly important [6–8].

As a low-density grinding media, ceramic balls are widely used in stirred mills because of their low specific gravity, good wear resistance, and iron contamination-free nature [9,10]. With technological breakthroughs, ceramic balls are now gradually entering ball mill applications. There have been a large number of related studies in the area of fine grinding. It has been proved that ceramic balls have a good grinding effect on the feed material with fine particle size and have a significant energy-saving effect. Zhang Xiaolong [11] studied the effect of cast iron and ceramic balls on the flotation kinetics

of chalcopyrite. The recovery of the milled product from cast iron balls was found to be lower than the recovery of the milled product from ceramic balls. Zhang et al. [12] found that the use of a ceramic ball medium avoided the excessive surface oxidation caused by the galvanic couple actions between an iron ball medium and sphalerite. It also proved that the chemical environment on the surface of sphalerite was optimized by the ceramic ball medium compared with the iron ball medium. Yuan et al. [13] found that the slurry mass concentration had a significant effect on ceramic balls grinding with magnetite. When the grinding concentration was higher than 50%, the breakage rate of magnetite plummeted to one-third of that at low mass concentrations. Fang et al. [14,15] described the first application of ceramic balls in an industrial mill, where the size distribution of the product obtained from ceramic ball grinding was significantly improved, and the overgrinding was reduced. A method of grinding ceramic balls and steel balls together was also introduced and yielded good energy saving and consumption reduction results. It was demonstrated that ceramic balls were able to achieve the same fineness as steel ball milling without reducing the mill's capacity, and reduced milling energy consumption by 51 per cent. However, in this case, the overall particle size of the mill feed is relatively fine. The -0.075 mm yield of the feed was 39.53%. Due to the harsh grinding conditions of ceramic balls, the grinding concentration, media filling rate, and ball diameter ratio have a large impact on them. In particular, ceramic ball milling has insufficient breakage capacity for coarse-grained ore particles [13]. The question remains: can ceramic balls be used in some mineral processing plants with a coarse feed size?

This study focused on the effect of adding steel balls to ceramic ball milling. Grinding comparison experiments were carried out under the same grinding conditions. The breakage rate of each grain size during grinding with three different grinding media, namely, steel balls, ceramic balls, and binary media, was analyzed by grinding kinetics.

2. Theoretical Background

2.1. Grinding Kinetics

Grinding kinetics reveals the laws of the particle size's characteristics in ground products with the change of time. By calculating the grinding kinetics, the breakage rates of different particle sizes during different times can be obtained. Then, the grinding pattern of each particle size class during the grinding process can be analyzed. The grinding kinetics formula is as follows [13,16,17].

$$R = R_0 e^{-kt^m} \quad (1)$$

Based on the grinding kinetics formula above, both sides of the formula are derived with respect to the time (t) to obtain the grinding speed.

$$\frac{dR}{dt} = R_0 e^{-kt^m} (-kmt^{m-1}) = -kmt^{m-1}R \quad (2)$$

In the formula, t is the grinding time. R is the yield of the discharge product greater than the specified particle size after the t . R_0 is the yield of the feed ore that is greater than the specified particle size. k and m are kinetic parameters that determine the nature of the ground material and the grinding conditions. Formula (2) is mathematically processed to give the following formula.

$$\ln\left(\ln\frac{R_0}{R}\right) = m \ln t + \ln k \quad (3)$$

Thus, in the coordinate system of $\ln t$ and $\ln\left(\ln\frac{R_0}{R}\right)$, the relationship between $\ln t$ and $\ln\left(\ln\frac{R_0}{R}\right)$ is a straight line with a slope m and an intercept $\ln k$, where the slope m represents the breakage rate. It should be noted, however, that this slope m can only represent the rate of breakage from milling time t_1 to milling time t_2 , $t_2 > t_1 > 0$. If we want to know the

grinding rate from grinding time 0 to t_1 , we need to compare the magnitude of $\ln\left(\ln\frac{R_0}{R}\right)$. The greater the $\ln\left(\ln\frac{R_0}{R}\right)$, the smaller the yield larger than the specified grain size [18–20].

2.2. Rosin–Rammler Particle Size Distribution

When the size of the milled product is fine, it is suitable to use the R–R distribution to describe the distribution of its particle size characteristics [21,22]. The R–R formula is as follows:

$$R = 100e^{-bx^n} \quad (4)$$

In the formula, R is the positive cumulative yield for particle sizes larger than x , %. x is the particle diameter or sieve width, mm. The parameter b is the parameter related to the product particle size. Parameter n is a parameter related to material properties. When $0 < x < 1$ mm, the smaller n is, the faster R decreases and the more uniform the particle size distribution [23,24].

3. Materials and Methods

3.1. Materials

The samples used in this experiment were sourced from the feed of the second-stage mill at the Washan concentrator of Nanshan Mining Co., located in Ma’anshan, Anhui, China. The plant employs a “stage grinding—stage separation” process, where each stage of the grinding operation is followed by a concentrator. This is set up to remove the monomer dissociated veinstone mineral, and the coarse concentrate is reground and recleaned in the next operation. The graph in Figure 1 illustrates the cumulative undersize distribution of the experimental samples. The yield of +0.3 mm is 34.68%, while the yield of −0.075 mm is 19.40%. The −0.075 mm yield is about half of Fangxin’s research material. This feed size is considered relatively coarse for ceramic ball milling [14], which is why it poses a challenge to use ceramic balls for grinding in second-stage mills in many iron ore mines. Therefore, this study aims to address the issue of the coarse feed size in the ceramic ball application process.

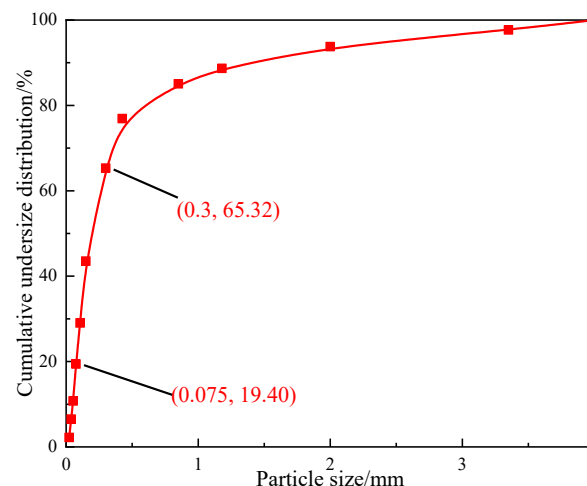


Figure 1. Cumulative undersize distribution of the feed.

3.2. Experimental Methods

The 500 g experimental samples were ground using an XMB270 × 90 mm wet ball mill from Wuhan Prospecting Institute (Wuhan, China), with a volume of 6.25 L and a speed of 96 r/min. Table 1 shows the physical properties of the two grinding media used in the experiments.

Table 1. Comparison of the parameters of ceramic balls and traditional steel balls.

Project	Steel Ball	Ceramic Ball
Main ingredients/%	Fe, Cr, C	Al, Si
Trace elements	Si, Mn, P, Mo, Al	Ca, Mg
Density/(t·m ⁻³)	7.3~7.8	3.7
Bulk density/(t·m ⁻³)	4.85	2.3
Mohs hardness	6.8	9.0
Self-wear/(g·(kg·h) ⁻¹)	60	5
Breakage ratio/%	≤0.5	≤0.1
Minimum effective diameter/mm	5	2

Experimental grinding tests were conducted to study the effect of different grinding media on grinding time. The tests were carried out under the same grinding conditions using three distinct grinding media regimes, namely, steel balls, ceramic balls, and binary media. All three grinding media were filled to 40% using the same ball size ratio, considering that the density of steel balls is almost twice that of ceramic balls, in order to be able to achieve significant energy savings. The binary media was filled with 30% porcelain balls and 10% steel balls. The volume ratio of ceramic balls to steel balls was 3:1. The experiments were conducted for 2, 4, 6, 8, and 10 min. The specific grinding conditions are presented in Table 2.

Table 2. Laboratory operating conditions.

Grinding Parameters	Specific Values					
Grinding Mass Concentration	67%					
Media Filling Ratio	40%					
Grinding Time	2 min, 4 min, 6 min, 8 min, 10 min					
Grinding Media	Steel Ball Size			Ceramic Ball Size		
	30 mm	25 mm	20 mm	30 mm	25 mm	20 mm
Steel Ball	2.425 kg	7.275 kg	2.425 kg	-	-	-
Ceramic Ball	-	-	-	1.1 kg	3.3 kg	1.1 kg
Binary Media	0.606 kg	1.819 kg	0.606 kg	0.825 kg	2.475 kg	0.825 kg

All the ground products were screened with a standard set of screeners (0.425 mm, 0.3 mm, 0.15 mm, 0.106 mm, 0.075 mm, 0.053 mm, 0.038 mm, and 0.023 mm). After 1 min of screening, the screening process was completed when the screened product was less than 1% of the mass fraction of the product remaining on the screener.

3.3. Energy Consumption Test

To monitor energy consumption during grinding, we tested the specific energy of grinding simultaneously and calculated it using the following formula [25–27].

$$E_{cs} = \frac{P \times T \times 60 \times 10^6}{M \times 3600} \quad (5)$$

$$P = P_1 - P_0 \quad (6)$$

where E_{cs} represents the specific energy, kWh/t. M represents the amount of grinding, g. T represents the grinding time, min. P represents the net input power of grinding, W. P_1 represents the input power of grinding, kW. P_0 represents the unloaded input power of grinding, kW.

4. Results and Discussion

4.1. Breakage Rate

Figure 2 shows the second-order grinding kinetics with different types of media, including steel balls, ceramic balls, and binary media. Figure 1a shows the results of fitting the grinding kinetics with steel balls for 2 to 10 min, consistent with second-order kinetics. It can be seen that the slope m of the primary function fitted for each particle size by steel ball milling is close, generally representing a rise–fall trend. As the size of the ore particles decreases, the energy required for breakage and crushing difficulty increases with higher particle strength [28,29]. On the other hand, the steel ball carries large kinetic energy. The impact breakage effect remains central while the grinding and stripping effect is a supplement during the grinding process. Therefore, the breakage rate decreases for fine-grained minerals, marking a slope m that decreases with the decrease of grain size.

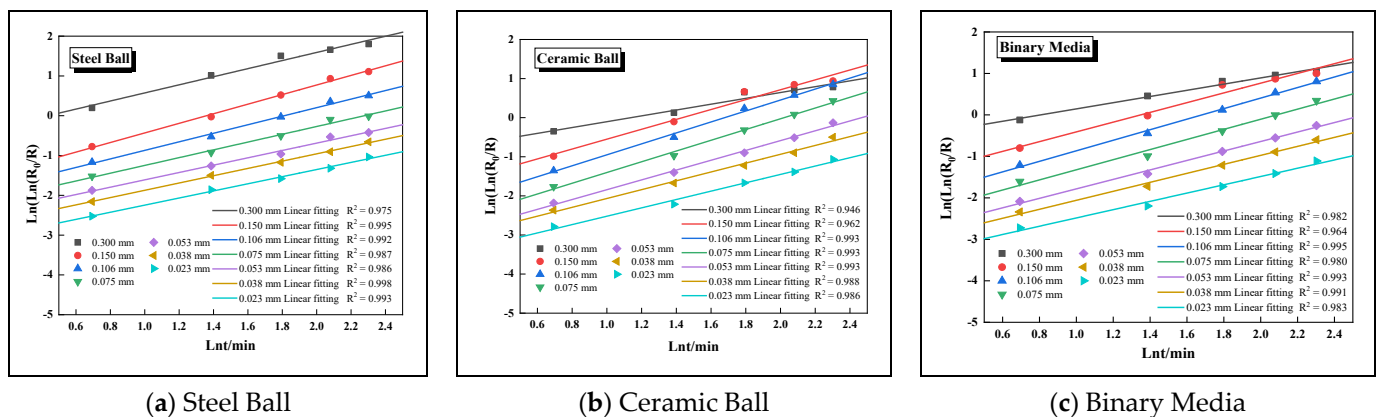


Figure 2. Second–order grinding kinetics fitting relationship for different media.

Figure 2b displays the results of the second-order grinding kinetics fit for ceramic ball grinding times of 2–10 min. The slope m trends upward and then downward. It has been observed that when the grinding media is changed from steel balls to ceramic balls, the breakage rate of larger 0.3 mm particles decreases [30]. This is because ore particles +0.3 mm require a high impact force to produce effective breakage.

The results of the second-order grinding kinetics fit with binary media during the grinding time of 2 min to 10 min are shown in Figure 2c. The overall trend exhibited is consistent with that of ceramic ball grinding, with the fine breakage rate higher than that of the coarse grains.

Table 3 shows the breakage rates of the three grinding media for each grain size at grinding times ranging from 2 to 10 min in detail. The breakage rate of the steel balls for 0.3 mm ore was 1.017, which was significantly higher than that of the ceramic balls, 0.746, and the binary media, 0.747. However, in the breakage rate of the other grain size, the steel balls are all lower than the ceramic balls and the binary media. This phenomenon is clearly inconsistent with the experimental results. This is because the results above reflect the breakage behavior from 2 min to 10 min of grinding time. However, the vast majority of the minerals in some grain classes are already crushed in the first 4 min, so when the grinding time is extended to 10 min, the breakage situation at each period cannot be accurately reflected [31,32].

The minimum size suitable for selecting most minerals in the industrial process is -0.075 mm. In addition, a -0.075 mm yield is also commonly used in China to express the fineness of the ore and as a measure of good grinding operations. In addition, due to the physical properties of ceramic balls, the specific gravity is small; in the grinding process of ceramic balls, the impact force is much smaller than that of steel balls. It is more difficult to cause effective impact breakage of coarser-grained ores. Taking these two points

together, this paper focuses on analyzing the breakage rate of +0.075 mm, which represents the fineness of the ore, and +0.3 mm, which represents the coarser grain size.

Table 3. Breakage rates of each grain size for the three grinding media at 2 to 10 min.

Particle Size/mm	Steel Ball	Ceramic Ball	Binary Media
0.300	1.017	0.746	0.747
0.150	1.204	1.264	1.174
0.106	1.073	1.401	1.271
0.075	0.978	1.374	1.218
0.053	0.923	1.256	1.142
0.038	0.916	1.130	1.083
0.023	0.894	1.069	0.998

Figure 3 shows the results of fitting the grinding kinetics for the three media regimes with the 0.3 mm grain size, with an adjustment of the fit range every two minutes. As can be seen from the graph, the highest trend line is for steel balls, followed by binary media, and the lowest trend line is for ceramic balls. The higher the trend line, the less of that particle size remains in the ground product. To put it simply, steel balls have a greater grinding effect on ore particles larger than +0.3 mm compared to ceramic balls [33,34]. However, when steel balls are added to the grinding process with ceramic balls, the combined effect improves significantly on particles larger than +0.3 mm. Although it is not as effective as using steel balls alone, it compensates for the limitations of ceramic ball milling to some degree.

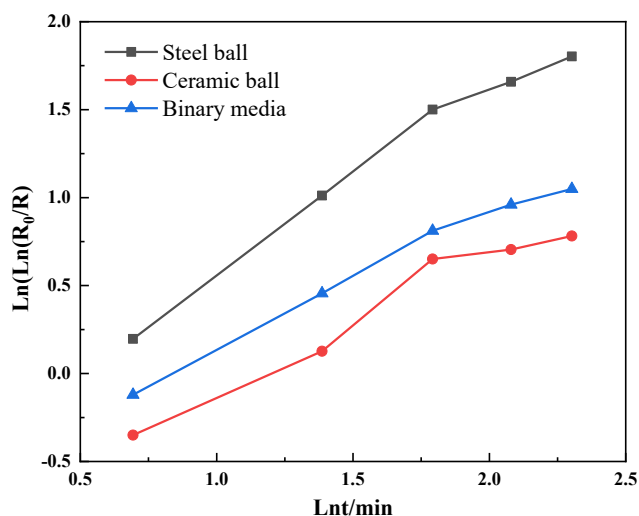


Figure 3. Results of the grinding kinetic fit for the 0.3 mm particle size.

Table 4 shows, in detail, the breakage rate of +0.3 mm ore for each time period for the three grinding media, where the breakage rate from 0 to 2 min is denoted by $\ln\left(\ln\frac{R_0}{R}\right)$. For the grain size of +0.3 mm, the breakage rate of steel balls is significantly higher than that of ceramic balls. After adding steel balls to the ceramic ball mill, it can make up half of the gap between ceramic balls and steel balls. It is interesting to note that at a grinding time of 4 to 6 min, the breakage rate of the ceramic balls is greater than that of the steel balls and the binary media. This is because the vast majority of the +0.3 mm ore is already ground when the grinding time reaches 4 min for the steel balls and binary media. It also can be found that all three grinding media have higher breakage rates for +0.3 mm ore at 0 to 6 min than at 6 to 10 min. This phenomenon indicates that most of the +0.3 mm ore is already ground in the first 6 min. In order to improve the grinding efficiency, the grinding time should be limited to 6 min.

Table 4. Breakage rates of +0.3 mm grain size for the three grinding media at 2 to 10 min.

Grinding Media	0–2 min ($\ln(\ln \frac{R_0}{R})$)	2–4 min	4–6 min	6–8 min	8–10 min
Steel ball	0.20	1.18	1.21	0.55	0.65
Ceramic ball	−0.35	0.69	1.29	0.19	0.34
Binary media	−0.12	0.83	0.88	0.52	0.40

Figure 4 shows the results of fitting the grinding kinetics for the three grinding media to 0.075 mm grain size, adjusting the fit range to every two minutes. As can be seen from the graph, the trend line for steel balls is significantly higher than that for ceramic balls and binary media during grinding times of 0 to 4 min. As the grinding time reaches 6 min, the trend line for ceramic balls is highest, followed by binary media and the lowest by steel balls, indicating that when the grinding time is extended to 6 min, the ceramic balls start to outperform the steel balls for the 0.075 mm grain size. After adding steel balls to the ceramic balls, the grinding effect is always between steel balls and ceramic balls. From 0 to 4 min, the grinding effect of the binary media is higher than that of ceramic balls but smaller than that of steel balls, and when the grinding time is extended to 6 min, the grinding effect of the binary media is higher than that of steel balls but smaller than that of ceramic balls.

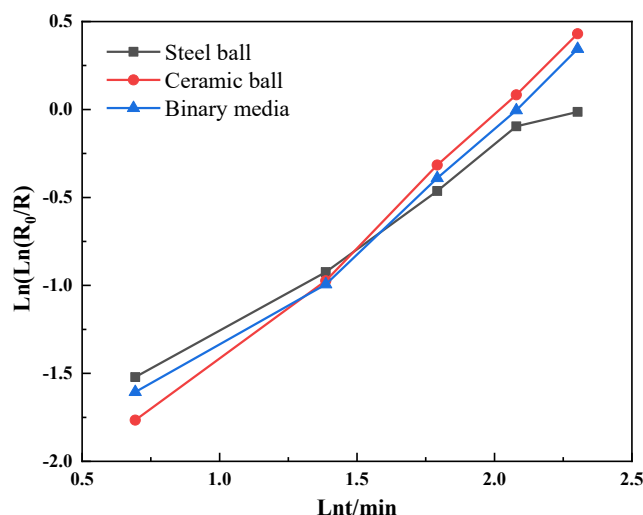


Figure 4. Results of the grinding kinetic fit for the 0.075 mm particle size.

Table 5 shows, in detail, the breakage rate of +0.075 mm ore for each time period for the three grinding media, where the breakage rate from 0 to 2 min is denoted by $\ln(\ln \frac{R_0}{R})$. At 2 to 4 min, the breakage rate of the steel balls was lower than that of the ceramic balls and binary media. It can be found that only at the time period from 0 to 2 min, the breakage rate of the steel balls is greater than that of the ceramic balls. In the time period from 2 to 10 min, the breakage rate of the ceramic balls is greater than that of the steel balls [11,35]. The pattern of change in the crushing rate of the binary media is consistent with that of the +0.3 mm grain size. Its breakage rate has been between that of steel balls and ceramic balls. This phenomenon shows that in the field of fine grinding, ceramic balls do have a superior grinding capacity. With the addition of steel balls to ceramic ball milling, this property is weakened, but is still higher than steel balls.

Table 5. Breakage rates of +0.075 mm grain size for each time period for the three grinding media.

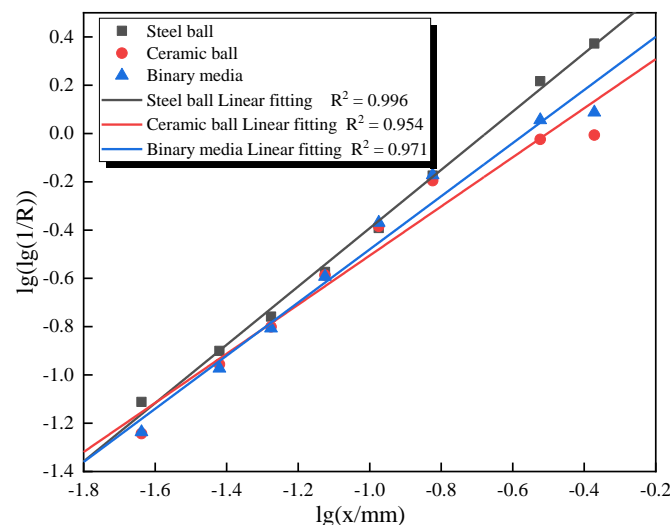
Grinding Media	0–2 min ($\ln(\ln \frac{R_0}{R})$)	2–4 min	4–6 min	6–8 min	8–10 min
Steel ball	−1.52	0.86	1.14	1.28	0.37
Ceramic ball	−1.77	1.14	1.62	1.39	1.56
Binary media	−1.61	0.88	1.49	1.34	1.56

In summary, at 0 to 10 min, the grinding effect of ceramic ball grinding for +0.3 mm particles is significantly lower than that of steel balls. The grinding effect for +0.075 mm particles is lower than that of steel balls when the grinding time is 0 to 4 min, but when the grinding time is more than 6 min, the grinding effect of the ceramic balls for +0.075 mm particles is better. It is possible to improve the grinding efficiency of ceramic balls by adding steel balls to compensate for the weakness of the ceramic balls in grinding particles with a size of +0.3 mm. Additionally, this method can also enhance the grinding ability of the ceramic balls on particles with a size of +0.075 mm during the first 4 min.

4.2. Particle Size Distribution

To be able to objectively compare the particle size characteristics of the ground products of the three grinding media, the ground products of the three grinding media at a grinding time of 4 min were compared.

Figure 5 shows the results of the fitting using the R–R formula for the three mill products. The vast majority of data points are on the line of fit, indicating a good fit.

**Figure 5.** Rosin–Rammler particle size distribution.

The magnitude of the parameter n can be obtained from the fitting results. The magnitude of parameter b can be obtained from further calculations. Table 6 demonstrates the specific values of parameter n and parameter b for the three mill products. In this batch of milling products, the most coarse grain size is +0.425 mm. Conforming to $0 < x < 1$ mm, at this time, the smaller n , the faster R falls, and the more uniform the particle size distribution [36,37]. The parameter n for the steel balls was the largest at 1.207, followed by the binary media at 1.101, and the ceramic balls' was the smallest at 1.017. That is to say, the ground product with ceramic balls has the most uniform particle size distribution, followed by the ground product with binary media, and the ground product with steel balls has the worst uniformity. This point can also illustrate that after replacing some of the ceramic balls with steel balls, although it can improve the breakage capacity of coarse grains, at the same time, it will also reduce the uniformity of the ground product.

Table 6. Parameter values of R–R formulas for three milled products.

Grinding Media	Parameter <i>n</i>	Parameter <i>b</i>	<i>R</i> ²
Steel ball	1.207	28.189	0.996
Ceramic ball	1.017	16.412	0.954
Binary media	1.101	19.032	0.971

Figure 6 illustrates the negative accumulation curves of the three ground products. In the fine-grained section, the negative cumulative particle size characteristic curve of the ceramic ball milling product and that of the steel ball milling almost coincide. This indicates that ceramic ball milling can also achieve the fineness of the steel ball milling. The −0.075 mm yield of the ceramic ball milling product is 44.90%, and the −0.075 mm yield of the steel ball milling product is 45.94%, and the difference between them is only 1.04 percentage point. For the coarse fraction, the grinding capacity of steel balls is significantly higher than that of ceramic balls. After adding steel balls to the ceramic ball milling, there was a significant increase in the negative accumulation curve of the ground product. This shows that this operation can make up for the shortcomings of the ceramic ball milling’s insufficient ability to grind coarse grains.

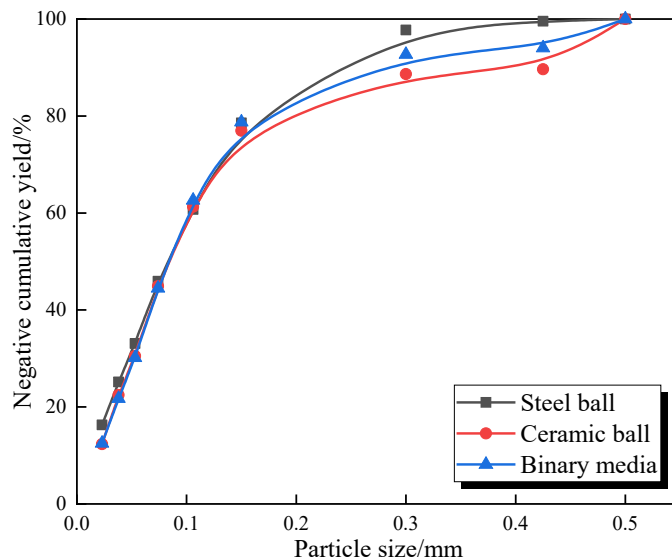


Figure 6. Cumulative undersize distribution of final productions based on three grinding methods.

4.3. Energy Consumption Distribution

Figure 7 illustrates the relationship between the amount of +0.3 mm ore remaining in the three mill products and the mill energy consumption. It can be seen that the grinding energy consumption of the steel balls is significantly higher than that of the ceramic balls and binary media. It also clearly shows that for the current experimental samples to be ground, based on the +0.3 mm residual of 25%, the energy consumption for steel ball milling is 11.661 kWh/t, for ceramic ball milling is 7.535 kWh/t, and for binary media milling is 9.003 kWh/h. Ceramic ball milling consumes 64.62% of the energy consumed by steel ball milling, and the energy consumption for binary media milling is 77.21% of the energy consumed by steel ball milling [38,39].

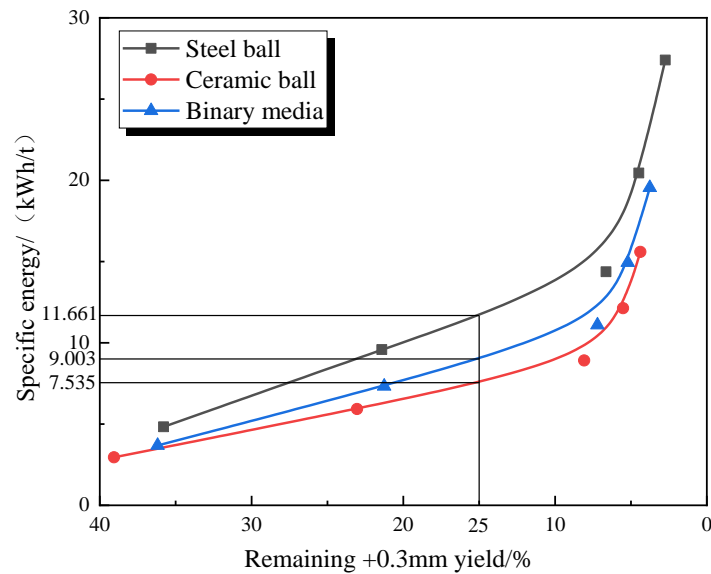


Figure 7. Relationship between remaining +0.3 mm yield and grinding energy consumption for three ground products.

Figure 8 demonstrates the relationship between the newly generated -0.075 mm yield of the three ground products and the grinding energy consumption. The new -0.075 mm yield is equal to the -0.075 mm yield of the mill product minus the -0.075 mm yield of the feed. We can find that the change rule of energy consumption demonstrated in Figures 6 and 7 is very similar, the energy consumption of steel ball grinding is significantly higher than that of ceramic ball grinding, and the energy consumption of grinding with binary media is in between them. Based on the newly generated -0.075 mm content of 45%, the energy consumption for grinding with steel balls is 18.709 kWh/t, for grinding with ceramic balls is 9.849 kWh/t, and for grinding with binary media is 12.973 kWh/t. The energy consumption for grinding with ceramic balls is 52.64% of the energy consumption for grinding with all steel balls. The grinding energy consumption of the binary media is 69.34% of that of the steel balls.

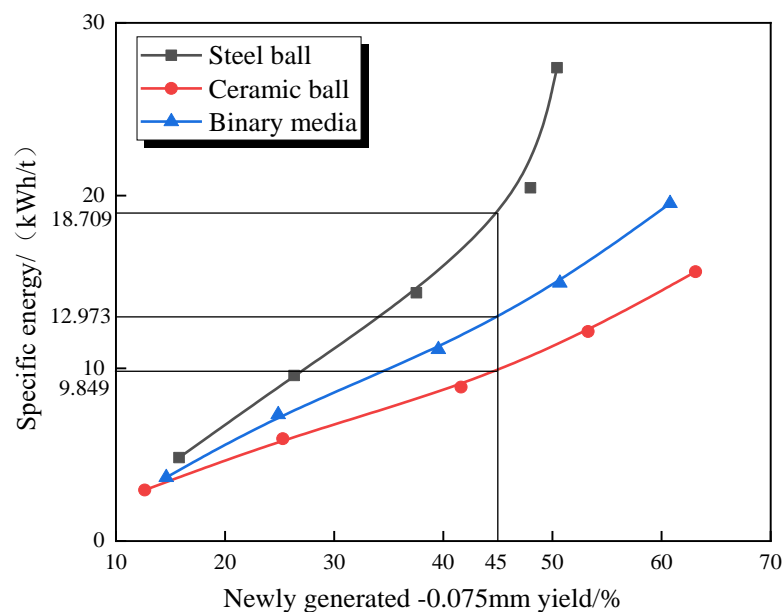
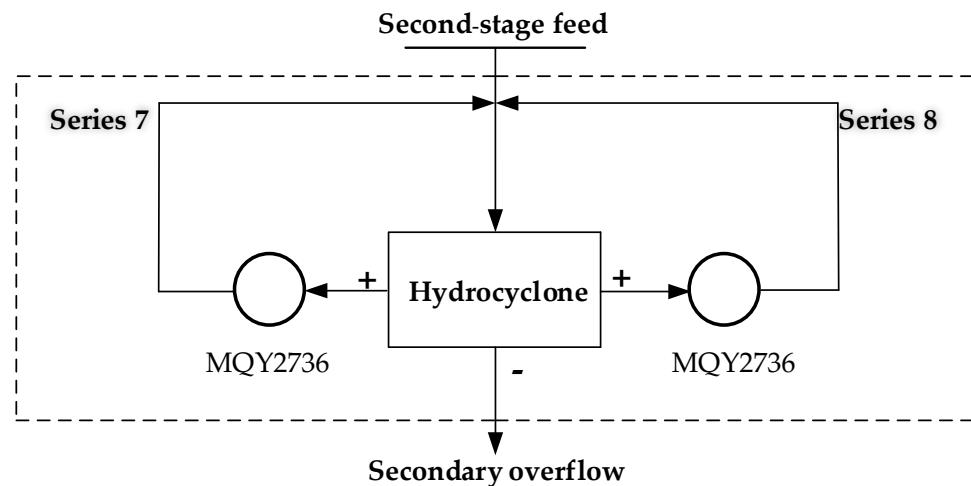


Figure 8. Relationship between newly generated -0.075 mm yield and grinding energy consumption for three ground products.

4.4. Industrial Applications

The Nanshan Mine is a common magnetite stage grinding-stage separation process. The product of the first-stage grinding and classifying system enters the first magnetic separation. The obtained coarse concentrate enters the second-stage grinding and classifying system. The second-stage classification system contains two MQY2700 × 3600 mm ball mills, and the two mills share a hydrocyclone unit. Both of the mills were produced from Sichuan Mining Machinery Co (Chengdu, China). The workflow is shown in Figure 9.



Note: + for coarse particles in the sinking sand, - for fine particles in the overflow.

Figure 9. Flow chart of the second-stage grinding and classifying of Washan processing plant.

Before the industrial experiment, both ball mills were ground with steel balls, and only $\Phi 50$ mm steel balls were used for loading and replenishing, with a filling rate of 33%. The experimental plan was to prioritize the modification of the #7 ball mill and the replacement of the mill media with ceramic balls, and then the modification and replacement of the grinding media for the #8 ball mill after the production of the concentrator stabilized.

At the beginning of the experiment, the #7 ball mill was loaded with ceramic balls, and the ratio of the ceramic ball was $\Phi 30$ mm: $\Phi 25$ mm: $\Phi 20$ mm = 3 t:9 t:3 t. Samples were taken from the #7 and #8 mill discharges, respectively, and the results are shown in Table 7.

Table 7. Mill #7/8 discharge product -0.075 mm production rate/%.

Grinding Media	Sample 1	Sample 2	Sample 3	Sample 4	Average
Mill #7 (Ceramic ball)	25.86	28.79	25.21	20.27	25.03
Mill #8 (Steel ball)	26.29	25.27	26.71	23.37	25.41

As can be seen from Table 7, the -0.075 mm yield of the ceramic ball grinding (mill #7) product is the same as the -0.075 mm yield of the steel ball grinding (mill #8) product, and the average fineness of -0.075 mm is very close between the ceramic ball and steel ball. This indicates that the replacement of steel balls with ceramic balls as the grinding media for the second stage of grinding is entirely feasible and will not affect the throughput of the processing plant. However, during the screening process, it was found that the ceramic ball ground product contained more coarse particles, which were subsequently screened at full particle size, and the main data is shown in Figure 9. It can be seen that the discharge yield of -0.075 mm was close to that of the ceramic ball mill ore and the steel ball mill ore, 24.58% and 25.81%, respectively. However, the ceramic ball ground product $+0.3$ mm yield is about 13 percentage points higher than that of the steel ball. This part of the coarse particles will re-enter the ball mill with the return sand, which will increase the load of the mill, and some limitations are confirmed in the industry that the ceramic ball is less effective in grinding the coarse particles.

Based on the initial findings of the industrial trials, a total of 1.5 tons of $\Phi 50$ mm steel balls were added to the #7 ball mill to increase the impact of the media on the coarse particles and thus enhance the grinding effect of the ball mill. After a period of stable operation with the addition of steel balls, the ground product was then sampled and screened. Figure 10 shows the particle size distribution of the ground product for the three different media regimes of ceramic ball, steel ball, and binary media. After the addition of steel balls to the #7 mill, the yield of coarse particles of +0.3 mm decreased significantly. The +0.3 mm yield in the ground product of the binary media was 13.45%, which was reduced by about 7 percentage points. Enhancing the grinding capacity of coarse particles by the addition of steel balls is a phenomenon consistent with what is seen in laboratory studies. This also indicates that the industrial application of ceramic balls may suffer from a lack of grinding capacity for coarse-grained minerals, which is a matter of concern.

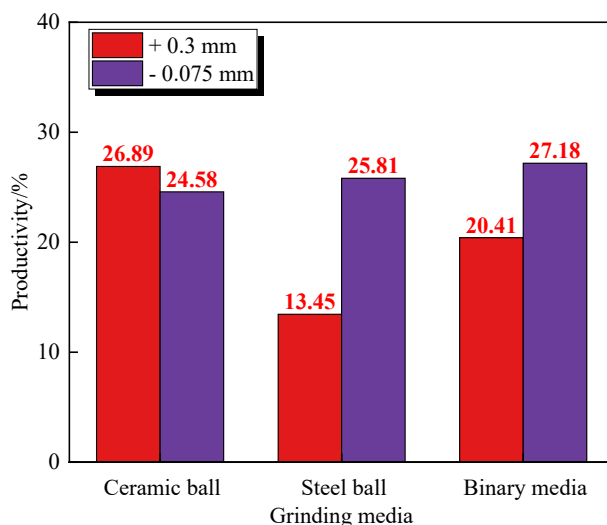


Figure 10. Ground products from industrial mills using three different grinding media.

In the later stages of the industrial experiment, both ball mills #7 and #8 replaced the grinding media from steel balls to ceramic balls and added a portion of steel balls after the production had stabilized. The mill and ball consumption were counted before and after the experiment.

Table 8 shows the specific situation of electricity and ball consumption before and after the industrial experiment. Without affecting the production capacity of the ore processing plant, the energy-saving and consumption-reduction effects of ceramic ball milling are remarkable. Compared with steel ball milling, the unit electricity consumption of ceramic ball milling decreased by 3.325 kWh/t, representing a decrease of 53.33%. The unit ball consumption cost decreased by 0.452 dollar/t, representing a decrease of 64.30%.

Table 8. Comparison of electricity consumption and ball consumption before and after the industrial experiment.

Project	Ceramic Ball	Steel Ball	Difference	Decrease/%
Electricity consumption/(kWh/t)	2.91	6.235	3.33	53.33
Ball consumption/(dollar/t)	0.251	0.703	0.45	64.30

5. Conclusions

The purpose of this study was to investigate how to improve the grinding effect of ceramic balls on coarse grains and make the ceramic balls adapt to coarser feed. Eventually, it can be applied to the majority of mines to achieve the purpose of saving energy and reducing consumption. To accomplish this, steel balls were incorporated into the ceramic

ball milling process, aiming to take advantage of the benefits of both methods. A grinding kinetics study was conducted using three different media options: steel balls, ceramic balls, and binary media.

The results show that ceramic balls are indeed even more excellent for grinding fine-grained grades. The breakage rate of ceramic ball milling for a +0.075 mm grain size is very close to that of steel ball milling. When the grinding time was extended to 6 min, the breakage rate of ceramic ball milling was higher than that of steel ball milling for the +0.075 mm grain size. However, ceramic ball milling does have some limitations for coarse grains, as well. The breakage rate of ceramic balls was less than that of steel balls for minerals of +0.3 mm grain size for the full time period.

The results show that adding steel balls to the ceramic balls improves the breakage efficiency of +0.3 mm ore in 0 to 10 min and +0.075 mm ore in 0 to 4 min. Although the binary media is still not as good as steel balls for breaking coarse grains, it was significantly improved, and it retains an excellent grinding ability for fine grain size; however, it reduces the homogeneity of the milled product. On the other hand, the binary media inherits the low energy consumption of ceramic balls. Industrial test results have shown that binary media can produce effective breakage of coarser feed material without reducing mill capacity, and it reduces electricity consumption by 53.33% and ball consumption by 64.30%. The results of industrial applications are consistent with the results of laboratory studies, which suggests that these conclusions are plausible.

In general, industrial second-stage mills usually use steel balls to grind the ore. However, with the advancement of material technology, ceramic balls can replace steel balls as the grinding media in second-stage mills. When the feed size fluctuation is large, such as in a magnetite ore processing plant in the second-stage mill, the feed volume and feed size will be affected by the grade of the original ore. Adding steel balls in the ceramic ball milling can achieve the grinding fineness requirements, and it also can produce significant energy saving and consumption reduction effects. It is a new grinding technology worth promoting and applying.

Author Contributions: Conceptualization, C.W. and Z.C.; methodology, N.L.; validation, C.Z.; formal analysis, Y.W.; investigation, J.T.; resources, Z.C.; data curation, Z.C.; writing—original draft preparation, Z.C.; writing—review and editing, C.W.; supervision, funding acquisition, C.W. and N.L. All authors have read and agreed to the published version of the manuscript.

Funding: This study was supported by the National Natural Science Foundation of China (grant number 51964016).

Data Availability Statement: The data presented in this study are available on request from the corresponding author, data available on request due to privacy.

Acknowledgments: The authors would like to thank the Jiangxi Key Laboratory of Mining Engineering and Anhui Nanshan Mining Co., Ltd., China, for their support. Yuexin Zheng from the Jiangxi University of Science and Technology is also gratefully acknowledged.

Conflicts of Interest: The authors declare no conflicts of interest.

References

1. Austin, L.G. Introduction to the mathematical description of grinding as a rate process. *Powder Technol.* **1972**, *5*, 1–17. [[CrossRef](#)]
2. Okay, A.; Tolga, S.; Deniz, A.; Alper, T.; Arno, K. Scale-up of Vertical Wet Stirred Media Mill (HIGmill) via Signature Plots, Stress Analyses and Energy Equations. *Miner. Eng.* **2024**, *205*, 108460.
3. Merkus, H.G.; Meesters, G.M.H. *Production, Handling and Characterization of Particulate Materials*; Springer: Berlin/Heidelberg, Germany, 2016; pp. 161–162.
4. Shi, F. A review of the applications of the JK size-dependent breakage model: Part 1: Ore and coal breakage characterization. *Int. J. Miner. Process.* **2016**, *155*, 118–129. [[CrossRef](#)]
5. Norgate, T.; Haque, N. Energy and greenhouse gas impacts of mining and mineral processing operations. *Clean Prod.* **2010**, *18*, 266–274. [[CrossRef](#)]
6. Wang, J.; Tian, Y.; Hu, X.; Han, J.; Liu, B. Integrated assessment and optimization of dual environment and production drivers in grinding. *Energy* **2023**, *272*, 127046. [[CrossRef](#)]

7. Adem, A. A comprehensive investigation of a grinding unit to reduce energy consumption, environmental effects and costs of a cement factory, a case study in Türkiye. *Energy Effic.* **2023**, *16*, 36.
8. Himani, S.; Murlidhar, M.; Pramod, P.K.; Nitin, K. Grinding characteristics and energy consumption in cryogenic and ambient grinding of ajwain seeds at varied moisture contents. *Powder Technol.* **2022**, *405*, 117531.
9. Zhang, X.; Qin, Y.; Jin, J.; Li, Y.; Gao, P. High-efficiency and energy-conservation grinding technology using a special ceramic-medium stirred mill: A pilot-scale study. *Powder Technol.* **2022**, *396*, 354–365. [[CrossRef](#)]
10. Zhang, X.; Han, Y.; Gao, P.; Li, Y. Effects of grinding media on grinding products and flotation performance of chalcopyrite. *Miner. Eng.* **2020**, *145*, 106070. [[CrossRef](#)]
11. Zhang, X.; Han, Y.; Sun, M.; Wen, B.; Li, Y.; He, J. Insight into the effects of grinding media on the flotation kinetics of chalcopyrite. *Adv. Powder Technol.* **2022**, *33*, 103860. [[CrossRef](#)]
12. Zhao, Q.; Yang, H.; Tong, L.; Ma, P.; Jin, R.; Zhang, Q. An Investigation into the Effects of Grinding Medium on Interface Characteristics and Flotation Performance of Sphalerite in Cyanide System. *Minerals* **2022**, *12*, 1231. [[CrossRef](#)]
13. Yuan, C.; Wu, C.; Fang, X.; Liao, N.; Tong, J.; Yu, C. Effect of Slurry Concentration on the Ceramic Ball Grinding Characteristics of Magnetite. *Minerals* **2022**, *12*, 1569. [[CrossRef](#)]
14. Fang, X.; Wu, C.; Yuan, C.; Liao, N.; Chen, Z.; Li, Y.; Lai, J.; Zhang, Z. Can ceramic balls and steel balls be combined in an industrial tumbling mill? *Powder Technol.* **2022**, *412*, 118020. [[CrossRef](#)]
15. Fang, X.; Wu, C.; Yuan, C.; Liao, N.; Yuan, C.; Xie, B.; Tong, J. The first attempt of applying ceramic balls in industrial tumbling mill: A case study. *Miner. Eng.* **2022**, *180*, 107504. [[CrossRef](#)]
16. Petrakis, E. Effect of Size-Distribution Environment on Breakage Parameters Using Closed-Cycle Grinding Tests. *Materials* **2023**, *16*, 7687. [[CrossRef](#)] [[PubMed](#)]
17. Antsiferov, S.I.; Bogdanov, V.S.; Bogdanov, N.E.; Voronov, V.P.; Sychev, E.A. Pulverization Kinetics in a Vibrational Mill. *Russ. Eng. Res.* **2023**, *43*, 1126–1128.
18. Liu, S.; Li, Q.; Song, J. Study on the grinding kinetics of copper tailing powder. *Powder Technol.* **2018**, *330*, 105–113. [[CrossRef](#)]
19. Liu, S.; Li, Q.; Xie, G.; Li, L.; Xiao, H. Effect of grinding time on the particle characteristics of glass powder. *Powder Technol.* **2016**, *295*, 133–141. [[CrossRef](#)]
20. Djamarani, K.M.; Clark, I.M. Characterization of particle size based on fine and coarse fractions. *Powder Technol.* **1997**, *93*, 101–108. [[CrossRef](#)]
21. Bu, X.; Chen, Y.; Ma, G.; Sun, Y.; Ni, C.; Xie, G. Differences in dry and wet grinding with a high solid concentration of coking coal using a laboratory conical ball mill: Breakage rate, morphological characterization, and induction time. *Adv. Powder Technol.* **2019**, *30*, 2703–2711. [[CrossRef](#)]
22. Khalilullah, T.; Hüseyin, I.; Eray, T.; Gizem, A.; Kemal, A.M.; Burak, U.; Mustafa, S. Effect of duration and type of grinding on the particle size distribution and microstructure of natural pumice with low pozzolanic reactivity. *Powder Technol.* **2023**, *428*, 118839.
23. Hanumanthappa, H.; Vardhan, H.; Mandela, G.R.; Kaza, M.; Sah, R.; Shanmugam, B.K.; Pandiri, S. Investigation on Iron Ore Grinding based on Particle Size Distribution and Liberation. *Trans. Indian Inst. Met.* **2020**, prepubl. [[CrossRef](#)]
24. Hou, Y.; Ding, Y.; Yin, W.; Yao, J. Influence of grinding kinetic parameters on grinding speed. *J. Northeast. Univ. (Nat. Sci. Ed.)* **2013**, *34*, 708–711.
25. Magnus, B. Empirical energy and size distribution model for predicting single particle breakage in compression crushing. *Miner. Eng.* **2021**, *171*, 107094.
26. Yu, J.; Sun, H.; An, Y.; Gao, P.; Zhang, X.; Han, Y. Energy conservation and consumption reduction in grinding operations through ceramic media stirring mill: An industrial validation test. *Powder Technol.* **2023**, *429*, 118943. [[CrossRef](#)]
27. Shi, F.; Xie, W. A specific energy-based ball mill model: From batch grinding to continuous operation. *Miner. Eng.* **2016**, *86*, 66–74. [[CrossRef](#)]
28. Liang, Y.; Deng, B.; Zhang, H.; Hu, Q.; Wu, J.; Zhao, Y.; Xu, Z. Research on the grinding characteristics of lignite based on grinding kinetics. *Int. J. Coal Prep. Util.* **2023**, *43*, 1721–1739. [[CrossRef](#)]
29. Camalan, M. Correlating common breakage modes with impact breakage and ball milling of cement clinker and chromite. *Int. J. Min. Sci. Technol.* **2020**, *30*, 901–908. [[CrossRef](#)]
30. Gupta, V.K. Effect of particulate environment on the grinding kinetics of mixtures of minerals in ball mills. *Powder Technol.* **2020**, *375*, 549–558. [[CrossRef](#)]
31. Bürger, R.; Bustamante, O.; Fulla, M.R.; Rivera, I.E. A population balance model of ball wear in grinding mills: An experimental case study. *Miner. Eng.* **2018**, *128*, 288–293. [[CrossRef](#)]
32. Zhao, Q.; Yang, H.; Tong, L.; Jin, Z.; Jin, R. New Insights into Improving the Physicochemical Properties and Flotation Behavior of Pyrite Interfaces from Cyanide Tailings. *J. Sustain. Metall.* **2023**, *9*, 1155–1167. [[CrossRef](#)]
33. Guo, W.; Gui, X.; Xing, Y.; Zhang, H.; Ma, R.; Meng, W.; Luo, M. Study on the unequal-probability comminution of spodumene and feldspar during the grinding process of lithium ore. *Powder Technol.* **2023**, *418*, 118308. [[CrossRef](#)]
34. Gupta, V.K. Population balance modeling approach to determining the mill diameter scale-up factor: Consideration of size distributions of the ball and particulate contents of the mill. *Powder Technol.* **2022**, *395*, 412–423. [[CrossRef](#)]
35. Kotake, N.; Kuboki, M.; Kiya, S.; Kanda, Y. Influence of dry and wet grinding conditions on fineness and shape of particle size distribution of product in a ball mill. *Adv. Powder Technol.* **2010**, *22*, 86–92. [[CrossRef](#)]
36. Paul, M. Analysis and graphical representation of particle size distributions. *Powder Technol.* **2023**, *420*, 118100.

37. Zhou, W.; Han, Y.; Li, Y.; Yang, J.; Ma, S.; Sun, Y. Research on prediction model of ore grinding particle size distribution. *J. Dispers. Sci. Technol.* **2020**, *41*, 537–546.
38. Barış, A.; İhsan, T.; Mehmet, B. Studying the effect of different operation parameters on the grinding energy efficiency in laboratory stirred mill. *Adv. Powder Technol.* **2020**, *31*, 4517–4525.
39. Bouchard, J.; Desbiens, A.; Poulin, É. Reducing the energy footprint of grinding circuits: The process control paradigm. *IFAC PapersOnLine* **2017**, *50*, 1163–1168. [[CrossRef](#)]

Disclaimer/Publisher’s Note: The statements, opinions and data contained in all publications are solely those of the individual author(s) and contributor(s) and not of MDPI and/or the editor(s). MDPI and/or the editor(s) disclaim responsibility for any injury to people or property resulting from any ideas, methods, instructions or products referred to in the content.